nature

BRIEF COMMUNICATIONS

Rare items often missed in visual searches

Errors in spotting key targets soar alarmingly if they appear only infrequently during screening.

Our society relies on accurate performance in visual screening tasks — for example, to detect knives in luggage or tumours in mammograms. These are visual searches for rare targets. We show here that target rarity leads to disturbingly inaccurate performance in target detection: if observers do not find what they are looking for fairly frequently, they often fail to notice it when it does appear.

Visual search is the subject of voluminous lab literature[1]. Typically, observers perform several hundred searches and targets are presented on 50% of trials. But target prevalence in baggage checks or cancer screening is much lower (about 0.3% in routine mammography[2]).

We compared performance on high- and low-prevalence versions of an artificial baggage-screening task in which observers looked for 'tools' among objects drawn from other categories. Semi-transparent objects were presented against noisy backgrounds and were sometimes overlapping; the number of objects in a display was 3, 6, 12 or 18; target prevalence was 1%, 10% or 50%. (For methods, see supplementary information.)

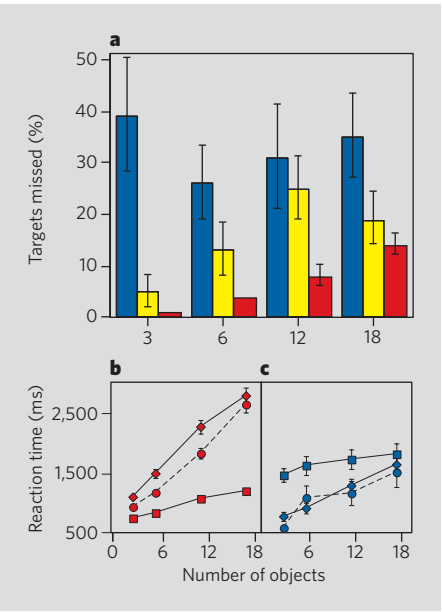

Figure 1 | The effects of target prevalence on search performance. **a**, Error rates for rare targets (blue bars, 1% prevalence), less rare targets (yellow bars, 10% prevalence) and common targets (red bars, 50% prevalence). Data from 12 observers are averaged. Error bars show ± s.e.m. for those 12 error rates. **b**, Reaction times for 50% prevalence. Typical reaction times are longer when the target is absent (circles) than when targets are present (squares). Diamonds show miss-error reaction times. **c**, Reaction times for 1% prevalence. At low prevalence, 'absent' responses are faster than 'present' responses. This leads to increased error rates. Error bars show ± s.e.m.

In the 1%-prevalence condition, 12 paid volunteer observers were each tested over 2,000 trials (broken into 250-trial blocks) that included only 20 target-present trials. Each observer was tested over 200 trials in the 10% and 50% conditions. Observers were given feedback on their performance, which included a points system designed to emphasize the importance of finding the target. Low-prevalence search has some similarity to vigilance tasks in which observers wait for fleeting signals[3,4]; however, our search stimuli were continuously visible until observers chose to respond.

We measured error rates as a function of the number of objects (Fig. 1a). A prevalence of 50% produced 7% miss errors (failing to notice a target), which is typical for laboratory search tasks of this sort. However, errors increase dramatically and consistently as prevalence decreases: 10% prevalence produced 16% errors, and errors soared to 30% at 1% prevalence.

Errors were primarily 'misses'. False alarms (saying "yes" when targets are absent) were vanishingly rare (0.03%), despite incentives to produce the opposite response (see methods in supplementary information). Simply changing prevalence produced a fourfold increase in error rate. If similar effects occur in socially important searches, the implications are significant.

Why does this happen? The reaction-time data shown in Fig. 1b,c provide some clues. Observers require a threshold for quitting when no target has been found. This threshold is constantly adjusted: observers slow down after making mistakes and speed up after successes[5]. When targets are frequent, fast "no" responses will often lead to mistakes. As a result, "no" reaction times are slower than "yes" reaction times in a high-prevalence search (Fig. 1b). With infrequent targets, observers can successfully say "no" almost all of the time, driving down the quitting threshold. As seen in Fig. 1c, the result is a target-absent search that is too swift: observers abandon their search in less than the average time required to find a target.

The problem cannot be solved simply by adding pseudotargets to increase prevalence (for example, by asking baggage searchers to check for iPods as well as weapons). In a second experiment, we mixed common (44% prevalence), rare (10%), and very rare (1%) targets so that some target was present in 50% of trials. Here, observers missed just 11% of common targets, but 25% of rare targets and 52% of very rare targets (see supplementary information).

Is the prevalence effect just a by-product of a naive observer's unfamiliarity with the targets? In a separate investigation, we compared the miss-error rate for 4,000 trials at 1% prevalence (40 targets, 41% miss errors) with the miss-error rate for the first 100 trials at 34% prevalence (34 targets, 11% miss errors). It seems to be prevalence and not just the number of targets presented that is critical (see supplementary information).

Visual search is a ubiquitous human signal-detection task[6]. Heuristics that produce acceptable performance over a wide range of target prevalence may betray us at low prevalence. Because the experiments are burdensome, we do not have a clear idea whether these effects occur in the field[7,8]. A scoring system in the laboratory cannot duplicate the motivation to find a gun or a tumour, nor the motivation to move the check-in line along. And the training of laboratory volunteers differs from that of professionals. Nevertheless, there are sufficient similarities between laboratory and field to indicate that we should find out whether the large increases in error demonstrated here also occur in socially important search tasks.

Jeremy M. Wolfe*†, Todd S. Horowitz*†, Naomi M. Kenner*

*Visual Attention Laboratory, Brigham and Women's Hospital, Boston, Massachusetts 02139, USA

†Department of Ophthalmology, Harvard Medical School, Boston, Massachusetts 02114, USA

e-mail: wolfe@search.bwh.harvard.edu

1. Wolfe, J. M. in *Attention* (ed. Pashler, H.) 13–74 (Psychology Press, Sussex, UK, 1998).
2. Gur, D. *et al. J. Natl Cancer Inst.* **96,** 185–190 (2004).
3. Warm, J. S. in *Workload Transition: Implications for Individual and Team Performance* (eds Huey, B. M. & Wicken, C. D.) 139–170 (National Academy, Washington DC, 1993).
4. Mackworth, J. *Vigilance and Attention* (Penguin, Harmondsworth, UK, 1970).
5. Chun, M. M. & Wolfe, J. M. *Cogn. Psychol.* **30,** 39–78 (1996).
6. Palmer, J., Verghese, P. & Pavel, M. *Vision Res.* **40,** 1227–1268 (2000).

7. Kundel, H. L. in *Medical Imaging 2000: Image Perception and Performance* (ed. Krupinski, E. A.) 135–144 (2000).
8. Gur, D., Rockette, H. E., Warfel, T., Lacomis, J. M. & Fuhrman, C. R. *Acad. Radiol.* **10,** 1324–1326 (2003).

doi:435439a
Supplementary information accompanies this communication on *Nature*'s website.
Competing financial interests: declared none.

BOSE–EINSTEIN CONDENSATES

Microscopic magnetic-field imaging

Today's magnetic-field sensors[1] are not capable of making measurements with both high spatial resolution and good field sensitivity. For example, magnetic force microscopy[2] allows the investigation of magnetic structures with a spatial resolution in the nanometre range, but with low sensitivity, whereas SQUIDs[3] and atomic magnetometers[4] enable extremely sensitive magnetic-field measurements to be made, but at low resolution. Here we use one-dimensional Bose–Einstein condensates in a microscopic field-imaging technique that combines high spatial resolution (within 3 micrometres) with high field sensitivity (300 picotesla).

Trapped cold atoms are ideal magnetic sensors as they are very sensitive to changes in magnetic-field landscapes, even in the presence of large homogeneous offset fields. Density modulations in trapped thermal atomic clouds have already been used as a measure of magnetic field variation caused by irregular current flow in nearby conductors[5–8]. We have produced a versatile, high-resolution sensor based on Bose–Einstein condensates (BECs). Its sensitivity is not limited by the temperature T of the cloud, but is rather determined by the chemical potential μ of the condensate, which can be orders of magnitude lower than $k_B T$ (where k_B is Boltzmann's constant).

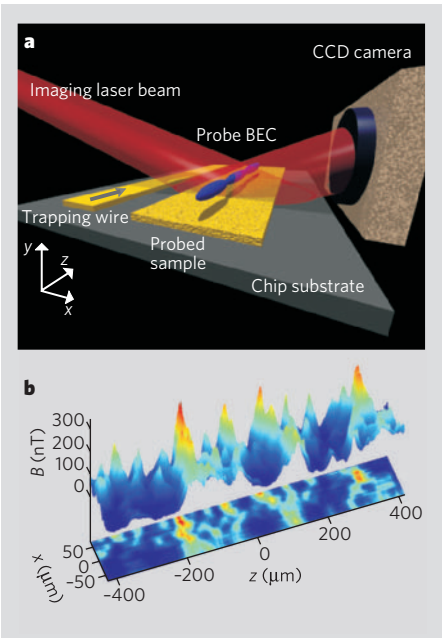

Figure 1 | One-dimensional Bose–Einstein condensate as a magnetic-field sensor. **a**, Experimental set-up. A Bose–Einstein condensate is created and trapped by a current-carrying wire mounted on a silicon surface (atom chip) and is positioned above the sample to be probed. **b**, Two-dimensional scan of the magnetic landscape (field component along the wire direction) above a 100-μm-wide and 3.1-μm-tall gold wire. This profile has been reconstructed from 28 equally spaced one-dimensional atomic-density traces measured 10 μm above the current-carrying wire at a homogeneous offset field of 2 millitesla, so that relative field variations of only 4 p.p.m. stemming from slightly irregular current flow could be measured at a spatial resolution of 3 μm.

The principles of the technique are shown in Fig. 1a. A BEC is trapped at the measurement site so that its density profile can be directly imaged. The spatially varying density is a measure of the potential energy and hence of the local magnetic-field variation. To probe spatial magnetic-field variations, we start by confining a one-dimensional BEC (in which μ is smaller than an energy quantum of transverse excitation)[9] in an elongated magnetic micro-trap with strong transverse and weak longitudinal confinement, created by small conductors mounted on the surface of an atom chip[10].

As a demonstration, we measured the magnetic-field variations above the 100-μm-wide current-carrying wire used to create the trap itself. Scanning the position of the BEC enabled us to reconstruct a full two-dimensional magnetic-field profile (Fig. 1b) near the wire with unprecedented accuracy (sensitivity of 4 nanotesla) at the measurement resolution (3 μm). From this map, we reconstructed the local current flow in the wire[11] and found extremely small angular deviations (2×10^{-4} root-mean-square radians) from a straight current path (for details, see supplementary information).

We also investigated an independent field landscape by placing a BEC close (5 μm) to a test wire structure. As long as this structure is grounded and carries no current, the atomic-density profile is homogeneous within the detection sensitivity. This corresponds to an upper bound in potential roughness of less than 10^{-14} eV, corresponding to a temperature of 200 picokelvin (field sensitivity of 300 picotesla). As soon as a small current (about 5 mA) is passed through the wire, a characteristic field profile is imaged.

The technique is applicable not only to magnetic fields, but can also be used to detect variations in electrostatic fields, as can be shown by charging the probed structure electrically. This measurement is more sensitive than the one discussed above because the trapping parameters can be adjusted independently from the measured potential landscape by using a separate wire for holding the BEC.

The optimal potential sensitivity of a BEC used as a field sensor, $\Delta B = \gamma \Delta N / z_0^3$, is achieved if the trapping parameters are adjusted so that the cloud's transverse size matches the desired spatial resolution z_0. Here ΔN is the minimal atom-number variation resolved by the imaging system, and γ contains all the atomic-physics parameters of the specific atom ($\gamma = 8.63 \times 10^{-29}$ tesla cubic metres for the ^{87}Rb used in our experiment). Currently available CCD (charge-coupled device) cameras allow atom-shot noise-limited detection with a ΔN value of better than 10 atoms per pixel in absorption imaging, so that a sensitivity, ΔB, of 1 nanotesla is possible even at a high spatial resolution of 1 μm (or 1 picotesla at 10 μm). By changing to a different atom with higher mass and/or by reducing the interatomic interaction, a significant increase in sensitivity can be achieved.

A comparison of different magnetic-field measurement techniques[1–4,12] (see supplementary information) shows that BECs as magnetic sensors could reach unprecedented sensitivity over a large range of spatial resolution. The sample measurements we present here reach higher sensitivities than those obtained with established techniques operating at the same spatial resolution.

Stephan Wildermuth*, Sebastian Hofferberth*, Igor Lesanovsky*, Elmar Haller*, L. Mauritz Andersson*, Sönke Groth*†, Israel Bar-Joseph†, Peter Krüger*, Jörg Schmiedmayer*
*Physikalisches Institut, Universität Heidelberg, Philosophenweg 12, 69120 Heidelberg, Germany
e-mail: schmiedmayer@atomchip.org
†Department of Condensed Matter Physics, The Weizmann Institute of Science, Rehovot 76100, Israel

1. Bending, S. J. *Adv. Phys.* **48,** 499–535 (1999).
2. Freeman, M. R. & Choi, B. C. *Science* **294,** 1484–1488 (2001).
3. Faley, M. I. *et al. Supercond. Sci. Technol.* **17,** 324–327 (2004).
4. Kominis, I. K., Kornack, T. W., Allred, J. C. & Romalis, M. V. *Nature* **422,** 596–599 (2003).
5. Fortagh, J., Ott, H., Kraft, S., Günther, A. & Zimmermann, C. *Phys. Rev. A* **66,** 041604 (2002).
6. Esteve, J. *et al. Phys. Rev. A* **70,** 043629 (2004).
7. Leanhardt, A. E. *et al. Phys. Rev. Lett.* **89,** 040401 (2002).
8. Jones, M. P. A. *et al. Phys. Rev. Lett.* **91,** 080401 (2003).
9. Dunjko, V., Lorent, V. & Olshanii, M. *Phys. Rev. Lett.* **86,** 5413–5416 (2001).
10. Folman, R., Krüger, P., Schmiedmayer, J., Denschlag, J. & Henkel, C. *Adv. At. Mol. Opt. Phys.* **48,** 263–356 (2002).
11. Rous, P. J., Yongsunthon, R., Stanishevsky, A. & Williams, E. D. *J. Appl. Phys.* **95,** 2477–2486 (2004).
12. Oral, A. *et al. IEEE Trans. Magn.* **38,** 2438–2440 (2002).

doi:435440a
Supplementary information accompanies this communication on *Nature*'s website .
Competing financial interests: declared none.

BRIEF COMMUNICATIONS ARISING online
www.nature.com/bca see Contents pages.